

Experimental Investigations of THz radiation from composite corrugated capillary with reflector

Channeling 2016, 25 – 30 Sept 2016.

K. Lekomtsev ^a, A. Aryshev ^b, A.A. Tishchenko ^c, A.A. Ponomarenko ^c, M. Shevelev ^b,
P. Karataev ^a, N. Terunuma ^b, J. Urakawa ^b

^a John Adams Institute at Royal Holloway University of London, Egham, UK

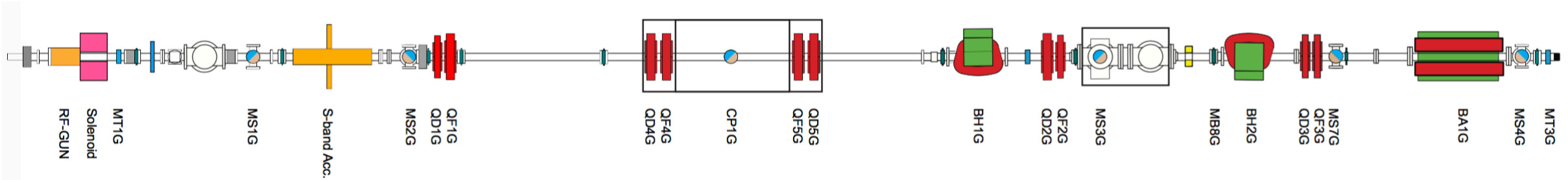
^b High Energy Accelerator Research Organization KEK, Tsukuba, Japan

^c National Research Nuclear University (MEPhI), Moscow, Russia

Introduction

1. Overview of the LUCX facility.
2. Cherenkov Smith – Purcell radiation (ChSPR) from corrugated capillary with reflector.
 - a. Brief theoretical background and comparison with simulations.
 - b. Particle In Cell simulations of the radiation from multi-bunch beam and capillary with reflector.
 - c. Discussion of experimental data.
3. Outlook
 - > Spectrum modulation on multi-bunch beam
 - > Drive – Witness, Beam modulation experiments with a new geometry.

LUCX facility: Overview



- The Laser Undulator Compact X-ray facility (LUCX) is a multipurpose linear accelerator which was initially constructed as an RF gun test bench and later extended to facilitate Compton scattering and coherent radiation generation experiments.

“Femtosecond mode”

- Ti:Sa laser
- e-bunch RMS length ~ 100 fs
- e-bunch charge < 100 pC
- Single bunch train, Micro-bunching 4-16 (4 is confirmed)
- Typical Rep. rate 3.13 Hz
- Experiments: THz program

“Picosecond mode”

- Q-switch Nd:YAG laser
- e-bunch RMS length ~ 10 ps
- e-bunch charge < 0.5 nC
- Multi-bunch train 2- few 10^3
- Max Rep. rate 12.5 Hz
- Experiments: Compton, CDR

Theory and simulation of THz radiation from corrugated channel

Spectral – angular distribution * of the radiation generated as a result of the point like electron passing through corrugated channel in infinite dielectric ($R \rightarrow \infty$):

$$\frac{d^2 W(\mathbf{n}, \omega)}{d\Omega d\hbar\omega} = \frac{\alpha}{(2\pi)^2} \frac{|\varepsilon(\omega) - 1|^2}{\sqrt{\varepsilon(\omega)}} \frac{1}{(1 + \gamma^2 \beta^2 \varepsilon(\omega) \sin^2 \theta)^2 \varphi^2} \frac{\sin^2(k\varphi d N/2)}{\sin^2(k\varphi d/2)} \times$$

$$\times |[\mathbf{n}, \mathbf{e}_z] \{ (e^{-ik\varphi l} - 1)(F_1(r_1) - F_1(R)) + (e^{-ik\varphi d} - e^{-ik\varphi l})(F_1(r_2) - F_1(R)) \} +$$

$$+ \gamma[\mathbf{n}, \mathbf{e}_\perp] \{ (e^{-ik\varphi l} - 1)(F_2(r_1) - F_2(R)) + (e^{-ik\varphi d} - e^{-ik\varphi l})(F_2(r_2) - F_2(R)) \} |^2$$

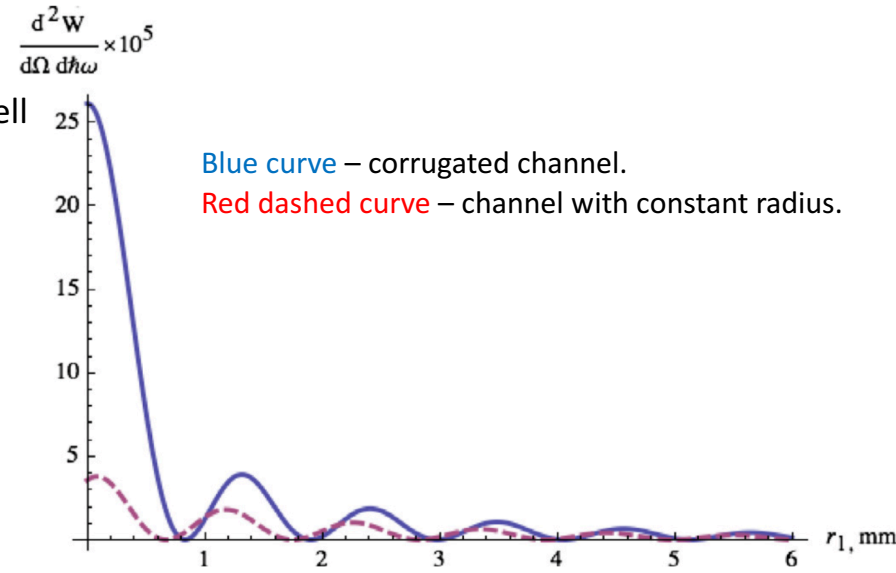
$$F_1(r) = -(kr \sin \theta) J_1(kr \sin \theta) K_0\left(\frac{kr}{\gamma\beta\sqrt{\varepsilon}}\right) + J_0(kr \sin \theta) \frac{kr}{\gamma\beta\sqrt{\varepsilon}} K_1\left(\frac{kr}{\gamma\beta\sqrt{\varepsilon}}\right)$$

$$F_2(r) = (kr \sin \theta) J_0(kr \sin \theta) K_1\left(\frac{kr}{\gamma\beta\sqrt{\varepsilon}}\right) + J_1(kr \sin \theta) \frac{kr}{\gamma\beta\sqrt{\varepsilon}} K_0\left(\frac{kr}{\gamma\beta\sqrt{\varepsilon}}\right)$$

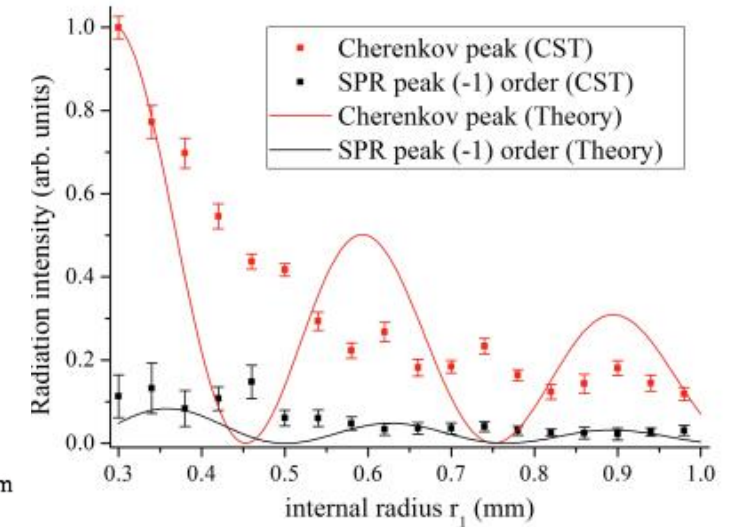
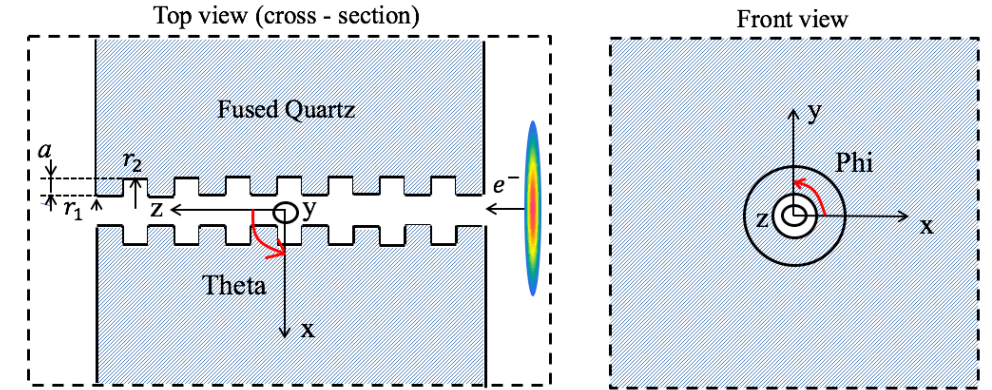
The diffraction orders of Cherenkov and Smith-Purcell radiation peaks satisfy the dispersion relation:

$$\cos(\theta) = \frac{2\pi m}{kd} + \frac{1}{\beta\sqrt{\varepsilon(\omega)}};$$

where θ is polar angle, β is the electron speed in terms of the speed of light, k is the wavenumber in dielectric, d is the corrugation period, m is a diffraction order, $\varepsilon(\omega)$ is dielectric permittivity as a function of frequency.

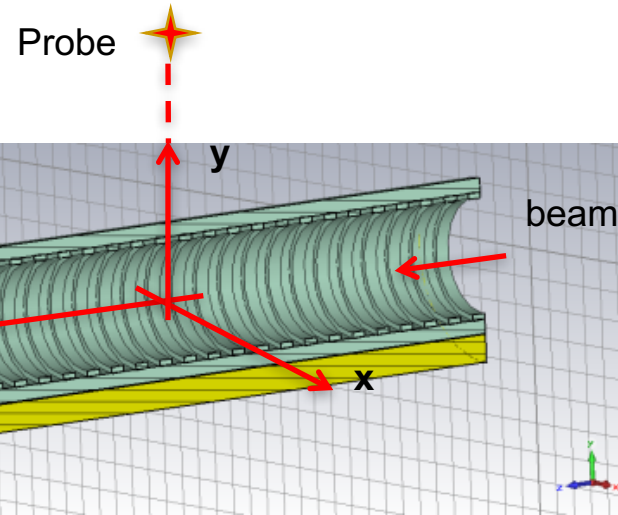


CST Particle In Cell simulation:

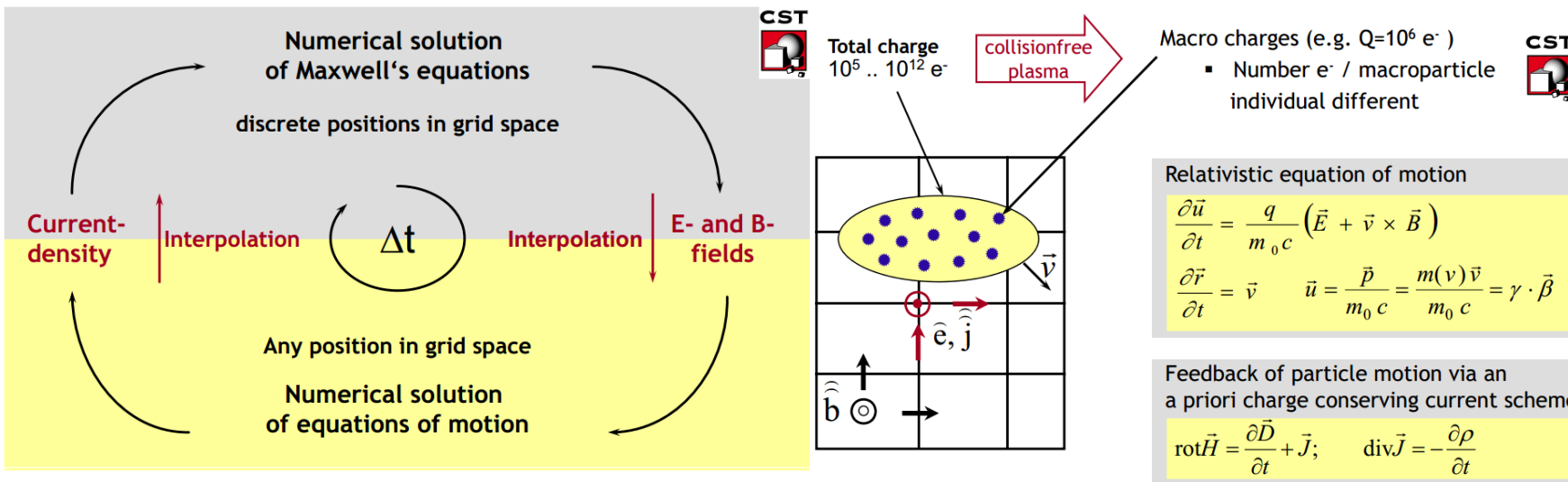


* A.A. Ponomarenko et. al, Terahertz radiation from electrons moving through a waveguide with variable radius, based on Smith-Purcell and Cherenkov mechanisms, NIMB 309, 223 (2013).

PIC simulations (capillary with reflector)



Simulation geometry (general view):

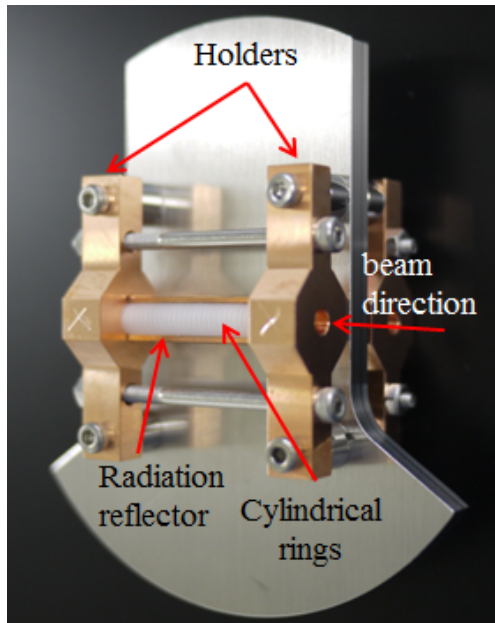


Parameter	Value
beam Lorentz - factor, γ	16
frequency	up to 700 GHz
bunch length, σ_{long}	~ 0.03 mm
bunch transverse size, σ_{transv}	~ 0.2 mm
micro-bunch charge	~ 0.1 nC
N of micro-bunches	4
distance between micro-bunches	variable (0.25 – 1 mm)
capillary material	Fused quartz
holder material	Copper
number of periods	30
cylindrical ring width, l	0.5 mm
corrugation period, $2l$	1 mm
groove depth, $r_2 - r_1$	0.2 mm
internal radius, r_1	2 mm
outer radius, r_3	2.7 mm

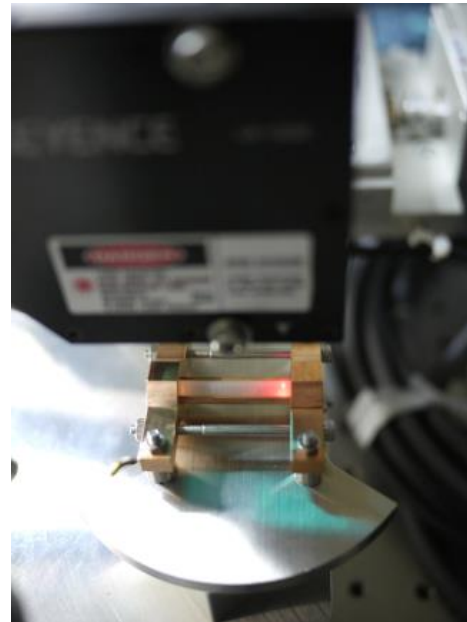
* Yee K S, Ingham D and Shlager K 1991 Time-Domain Extrapolation to the far field based on FDTD calculations *IEEE Trans. of Ant. and Prop.* **39** 410

Assembly of the capillary with holders

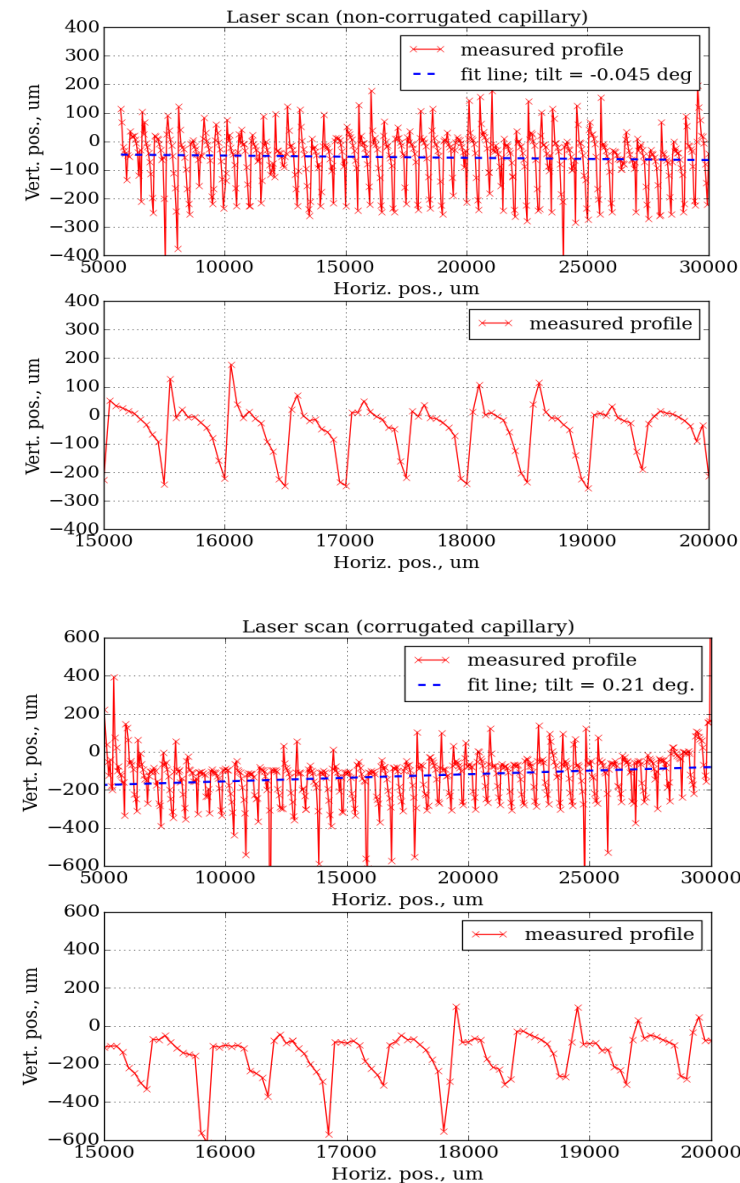
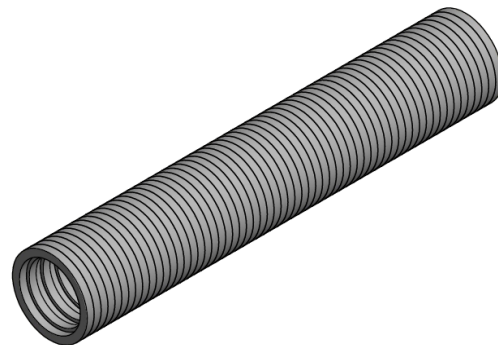
Capillary with holders and radiation reflector assembled on the base plate:



Laser scans were performed on the outside surface of the capillary installed in the holders:

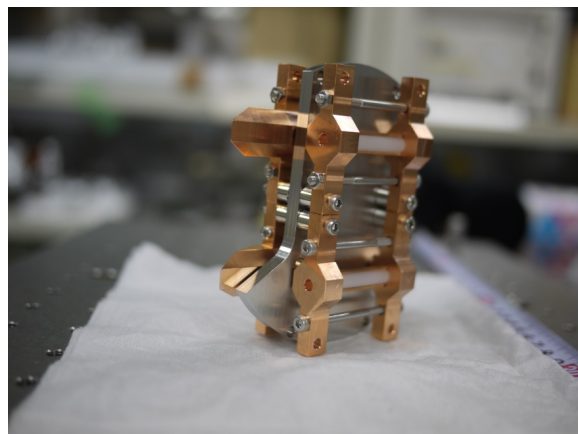
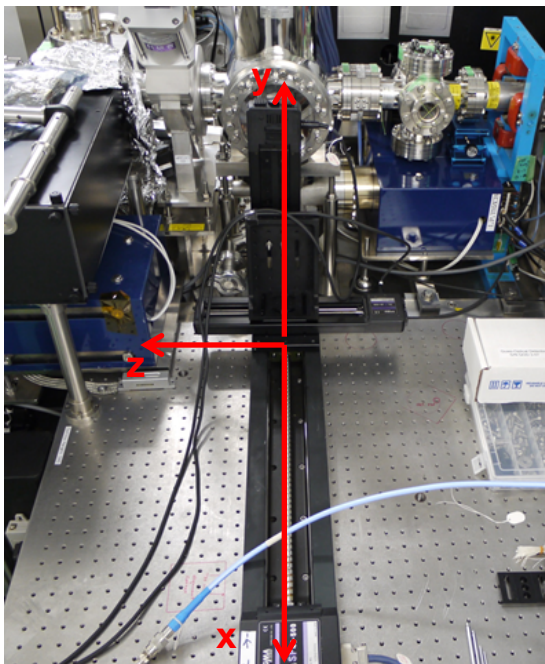


Both corrugated and blank capillaries are constructed as sets of cylindrical rings:



- Laser beam scanned along the outer surface of corrugated and blank capillaries.
- Light reflected from the surface detected by an array detector and the vertical offset of the laser beam recorder.
- As a result obtained the vertical offset as a function of the horizontal travel range.

Experiment (ChSPR)

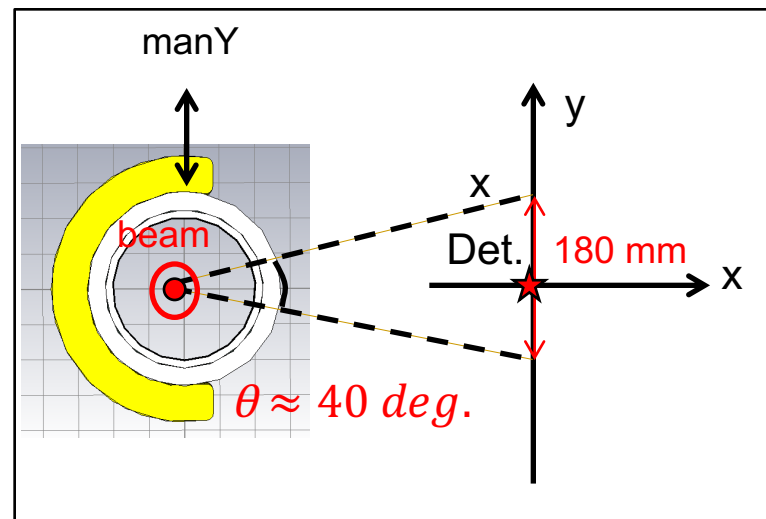
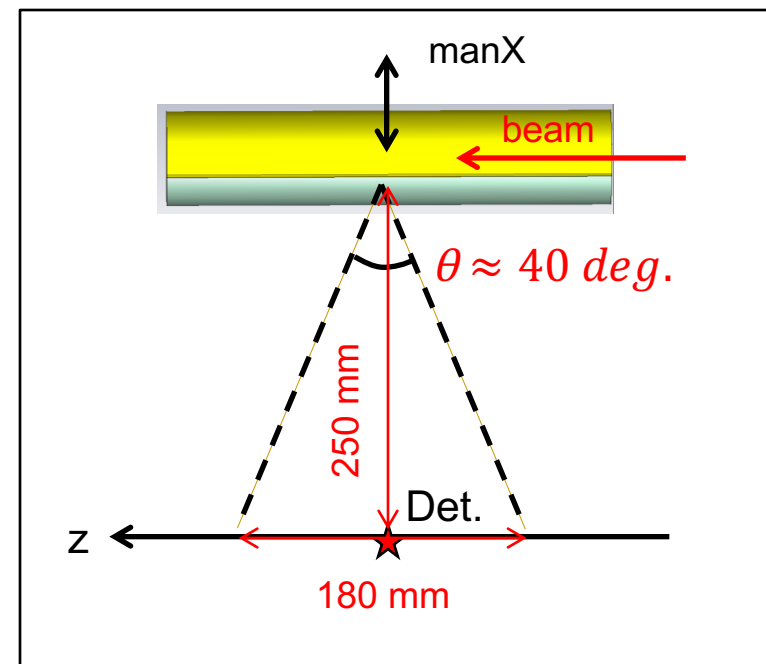
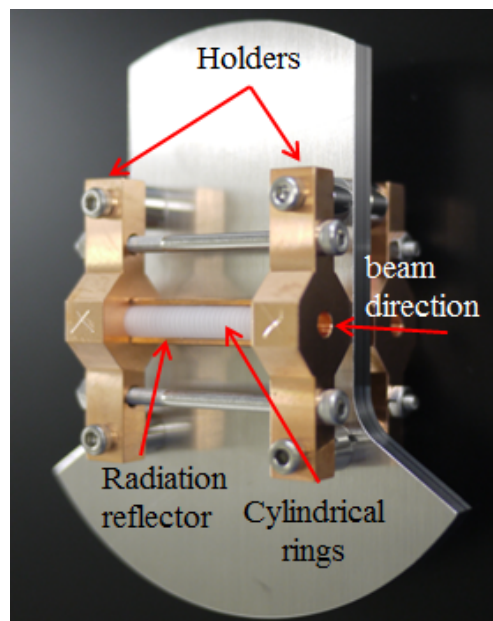


Bunch size:
 $200 \times 200 \mu\text{m}$

Bunch charge:
1 bunch 25 pC

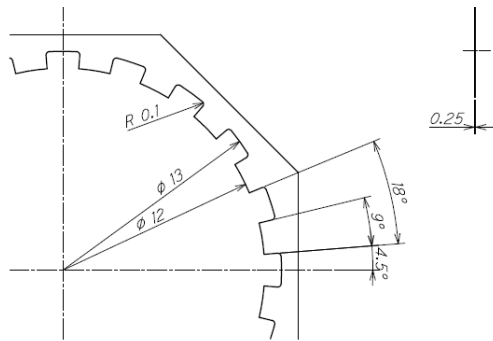
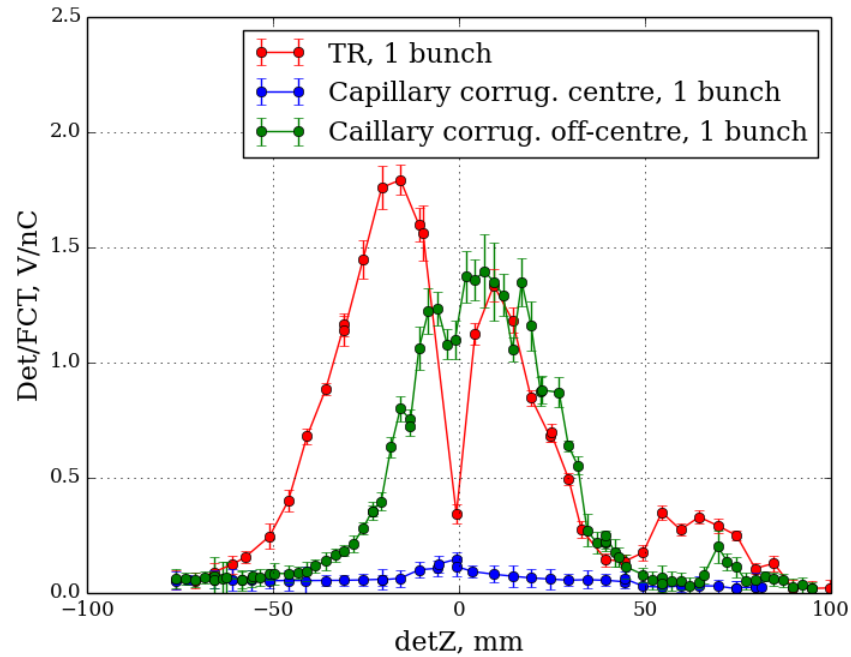
Detector:
SBD 320 – 460 GHz

Quartz vacuum window:
100 mm (effective diameter)

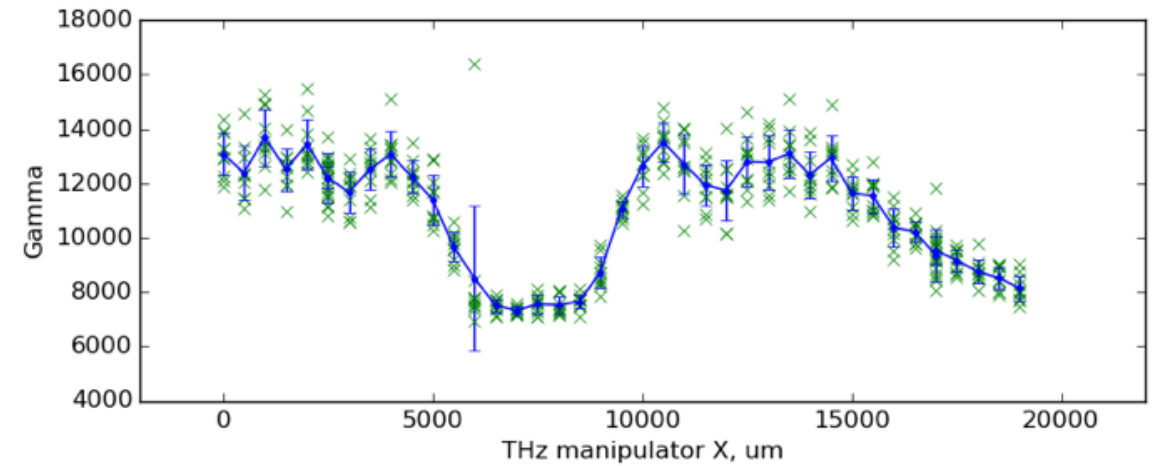
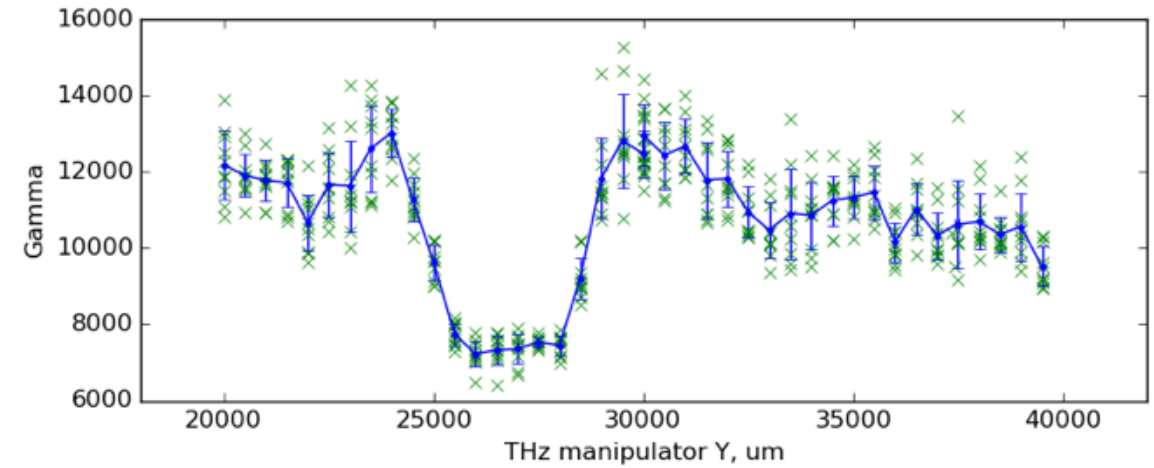


Experiment (ChSPR)

Cross-check with Transition radiation:

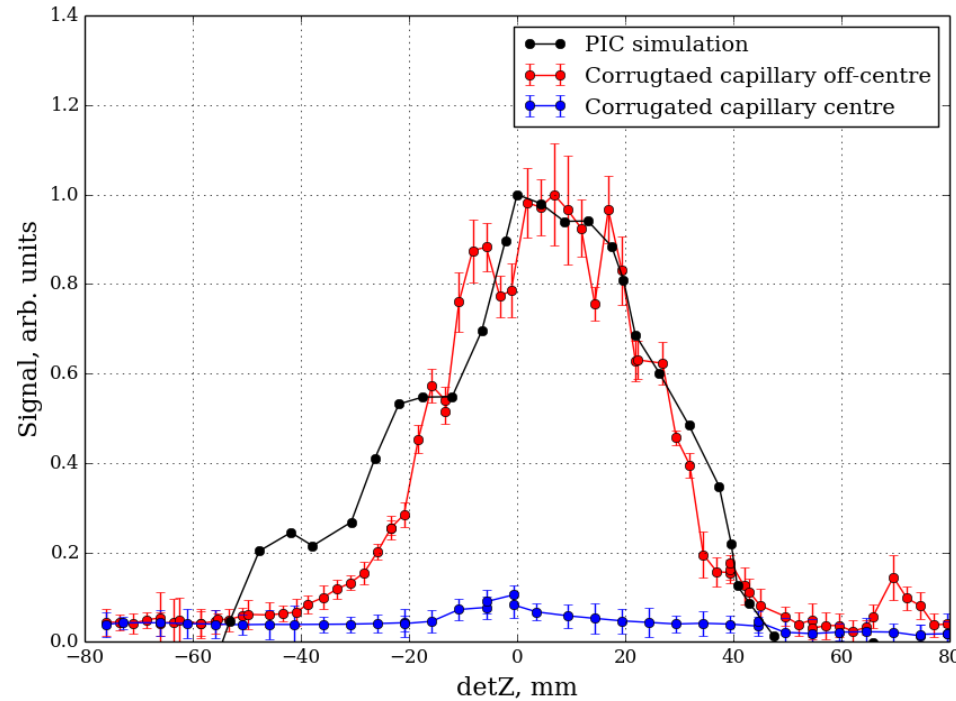
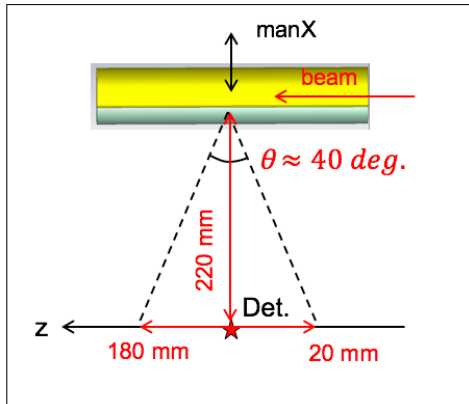


Positioning of the capillaries with respect to the beam
(bremsstrahlung, appearing due to direct interaction of the
electron beam with the target material):



Experiment (ChSPR)

Polar distribution of radiation:



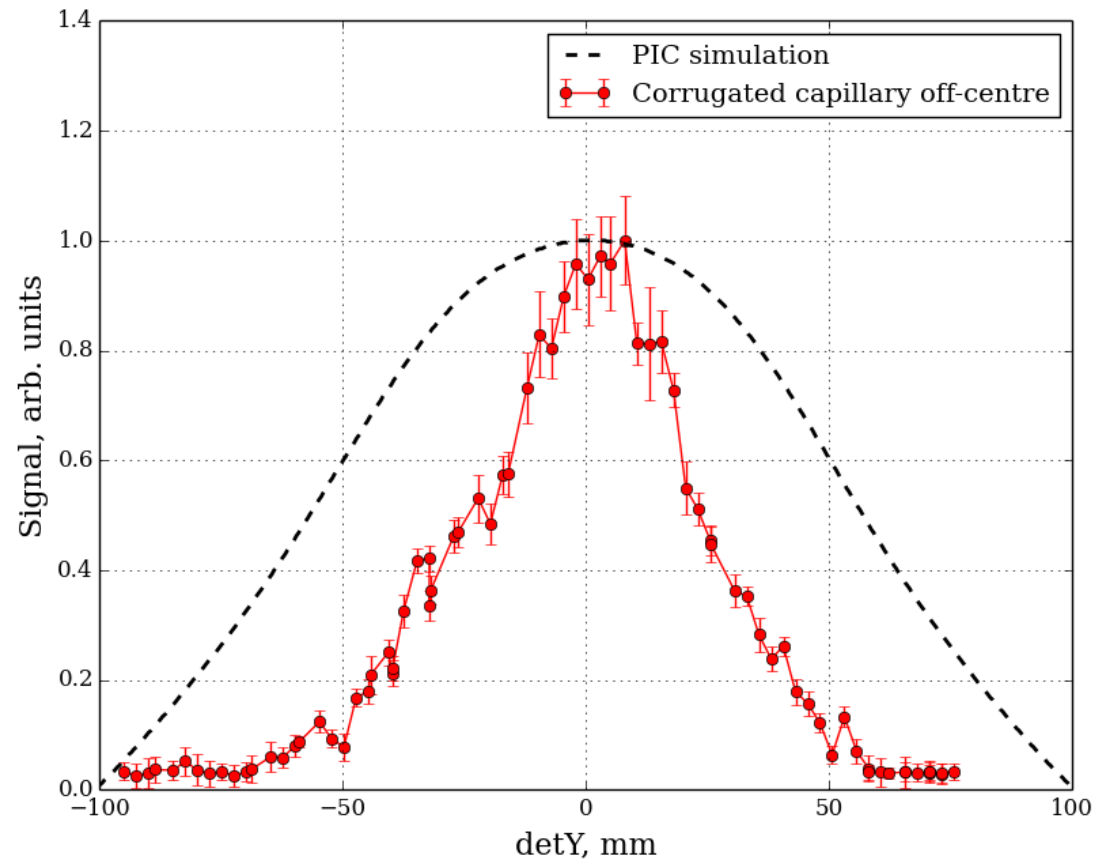
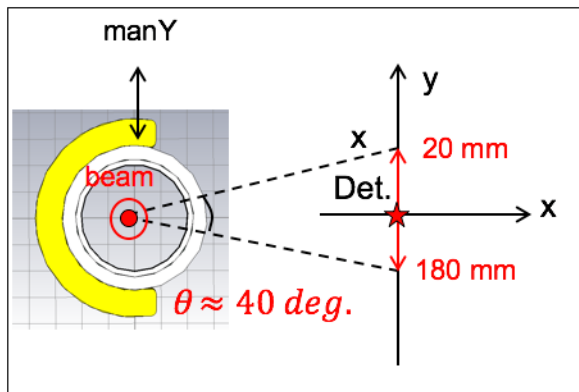
- The simulated geometry was identical to the realistic one with the exception of holders, which were not taken into account in the simulations.
- The beam parameters were chosen to be the same as during the time of the experiment, and the beam was moving at 0.6 mm from the corrugation to allow for 3σ beam – corrugation separation.
- The power distribution was obtained by, first, calculating the power spectrum of emitted radiation in the frequency range 240 – 360 GHz. The radiation directivity pattern for each frequency was calculated as well, hence it was possible to convert power spectrum into the power distribution at the detector locations on the translation stage.
- After the converted power distribution was obtained, the contribution of the blank capillary in the power spectrum was subtracted.
- The power spectrum of the radiation emitted through the surface of the outside boundary A of the calculation domain during the simulation time Δt was calculated as:

$$P(\omega) = \left| \int_0^{\Delta t} \oint \mathbf{S}(\omega) * \mathbf{n} dA dt \right|;$$

where $\mathbf{S}(\omega)$ is the Poynting vector, \mathbf{n} is a unity vector in the outward normal direction from the boundary A of the calculation domain.

Experiment (ChSPR)

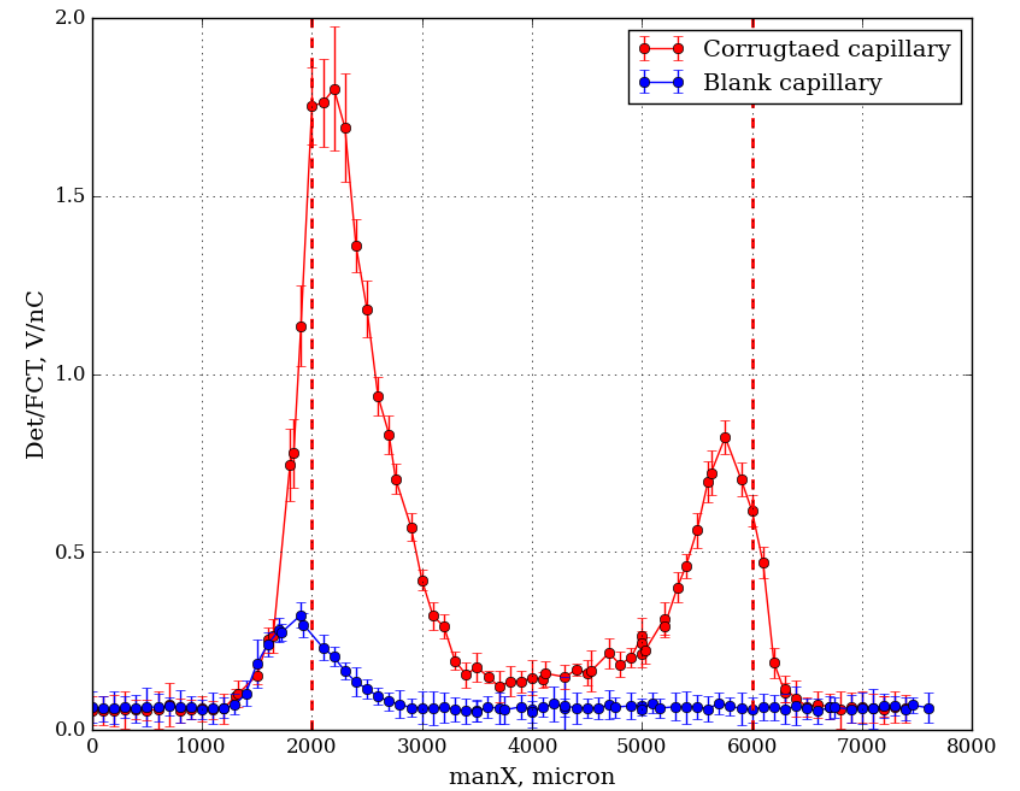
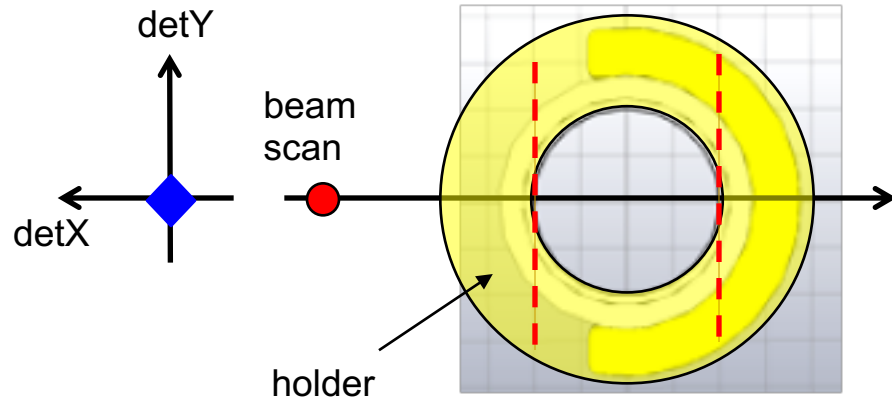
Azimuthal distribution of radiation:



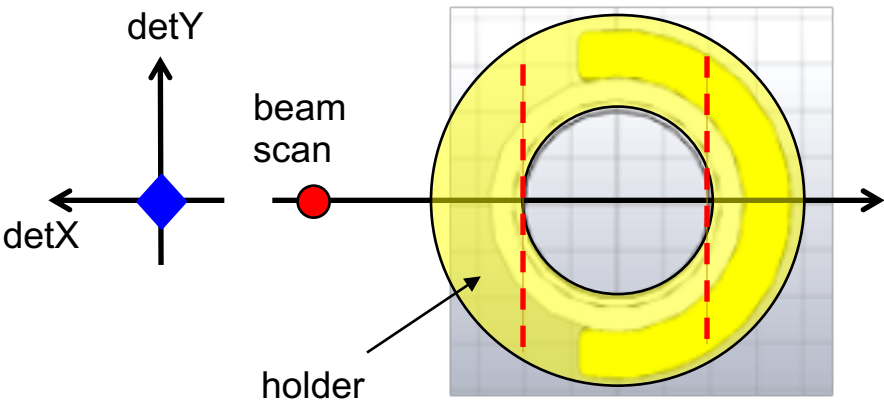
- Azimuthal distribution of the radiation was simulated using the [far-field monitor of CST Particle Studio](#), which extrapolates the electric field values at the border of the calculation domain to obtain the electric fields in the far-field (distances $\gg \gamma^2 \lambda$) at a single frequency.
- According to the dispersion relation: $\cos(\theta) = \frac{2\pi m}{kd} + \frac{1}{\beta \sqrt{\epsilon(\omega)}}$ the frequency at $\theta = 90 \text{ deg.}$ (detZ = 0) is 300 GHz ($\lambda = 1 \text{ mm}$).
- The red curve: [measurement of the azimuthal distribution of the radiation at 300GHz](#).

Experiment (capillary with reflector)

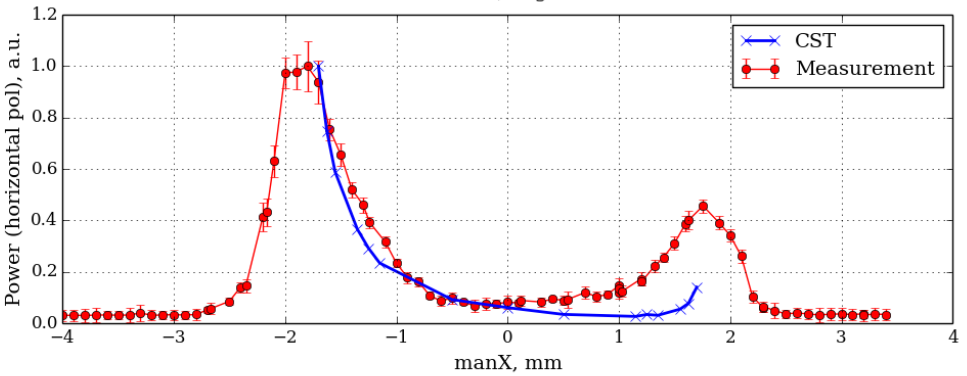
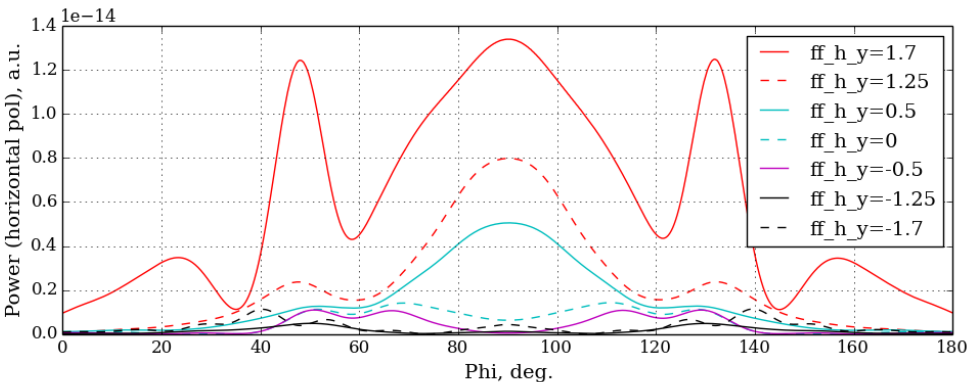
Target – beam separation and the corresponding radiation yield:



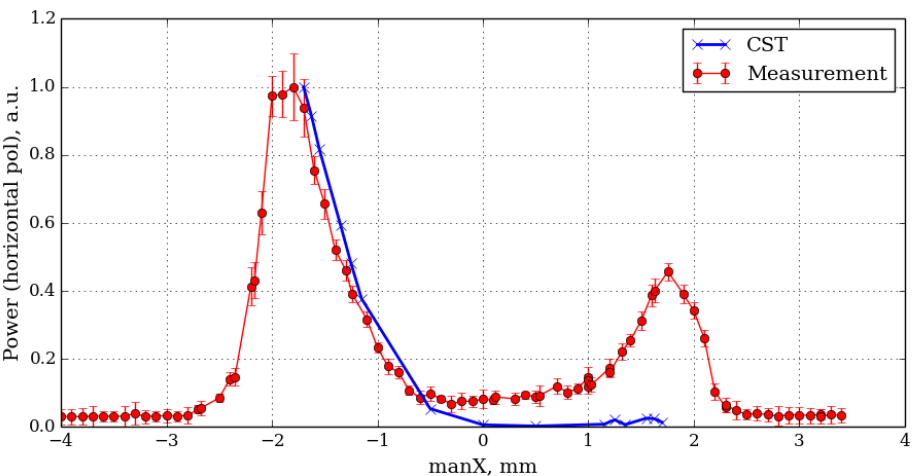
Experiment (capillary with reflector)



Farfield pattern at 300 GHz is integrated over the range of angles 0 – 90 deg. and compared with the measurement.



Integrated over the angular range 85 – 87 deg. (location of the detector):



Overview and outlook

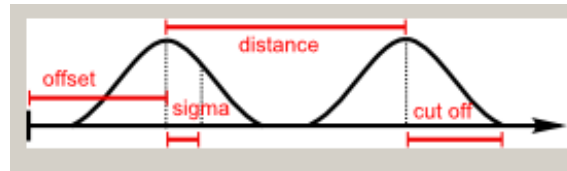
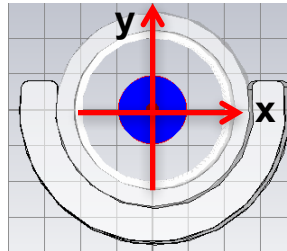
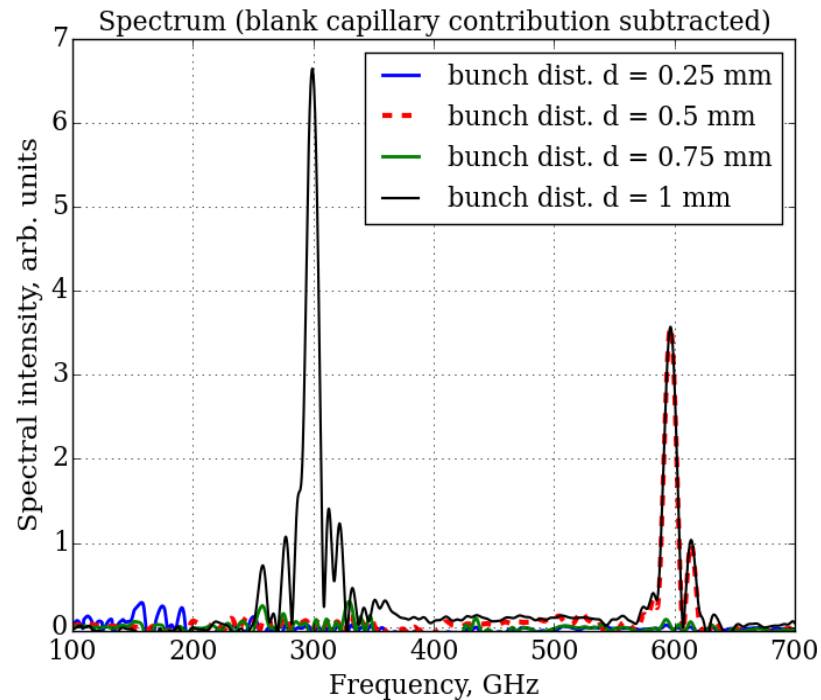
- The objectives of the ChSPR study were to cross-check the radiation with other well known radiation mechanism (TR), to study the effect of corrugation and measure the radiation distributions.
- Measured 10-fold increase of the radiation intensity for the corrugate capillary in comparison to the blank capillary.
- Confirmed that the maximum of the radiation intensity is achieved for the off-central beam propagation.
- The composite design of the corrugated capillary allows for flexibility to easily change the geometry, which can be very useful for a variety of studies including radiation generation, beam energy and charge modulation etc.

Outlook:

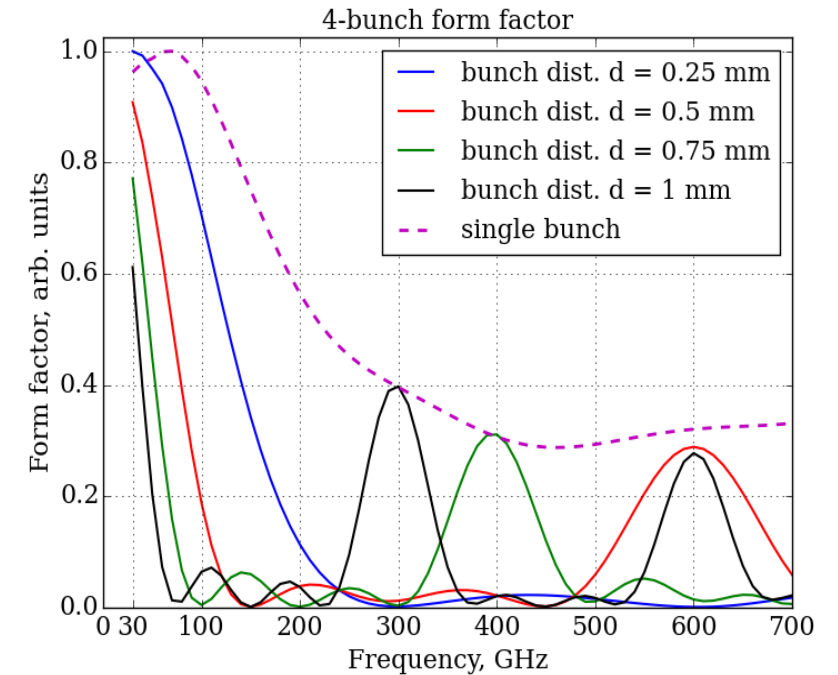
- > Spectrum modulation on multi-bunch beam
- > Drive – Witness, Beam modulation experiments with a new geometry.

PIC simulations multi-bunch (capillary with reflector)

Beam position: $x = 0$ mm, $y = 1$ mm



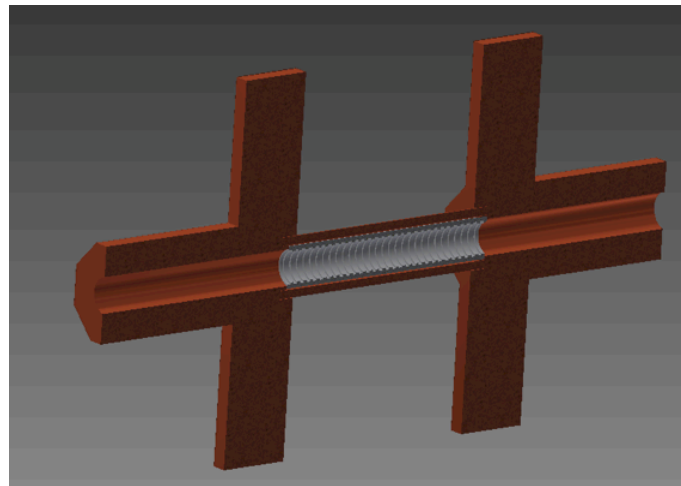
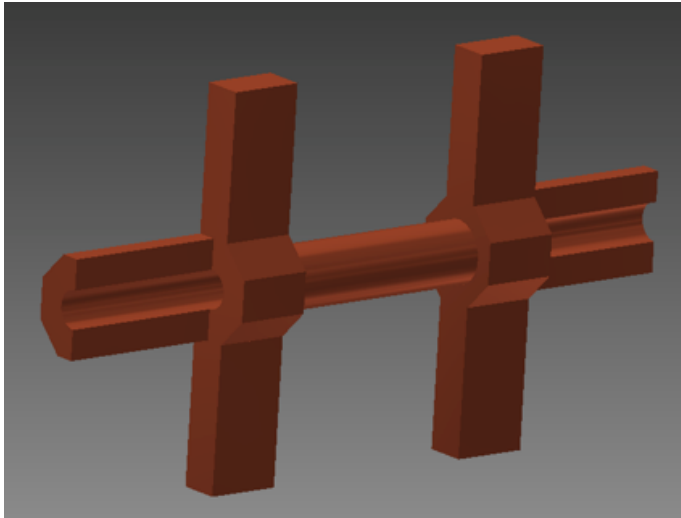
Form-factors of four bunches with different bunch spacing, and the form factor of a single bunch:



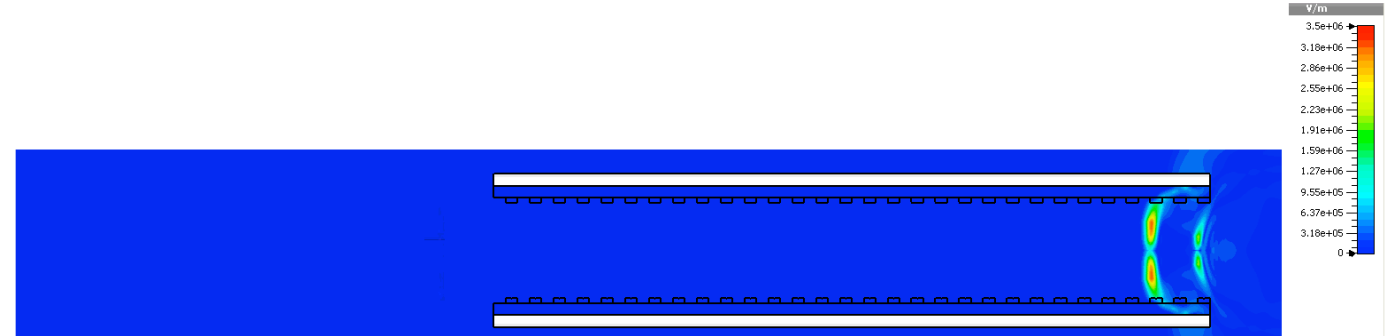
Spectral modulation of the radiation depends on the periodicity of the corrugation as well as the distance between bunches.

PIC simulations Drive-Witness experiment (new geometry)

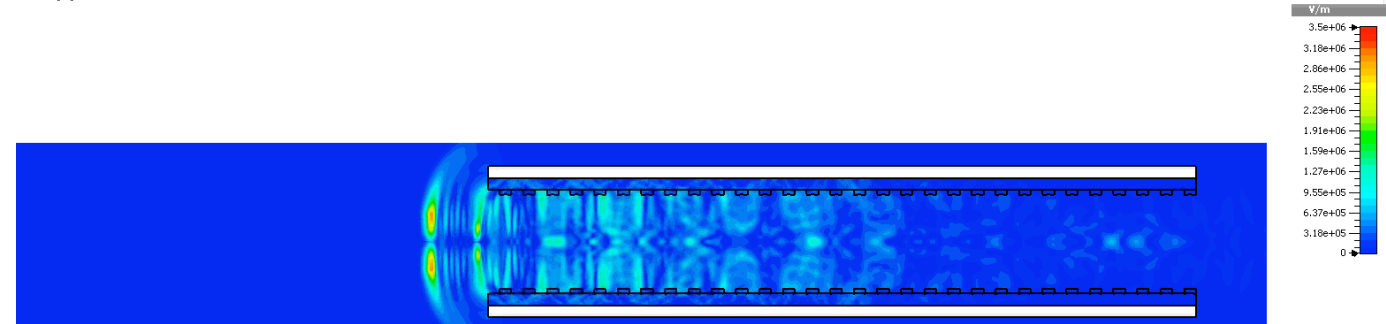
Modified holder design:



PIC simulation example for Drive (100pC) and Witness (20pC) separated by two corrugation periods:



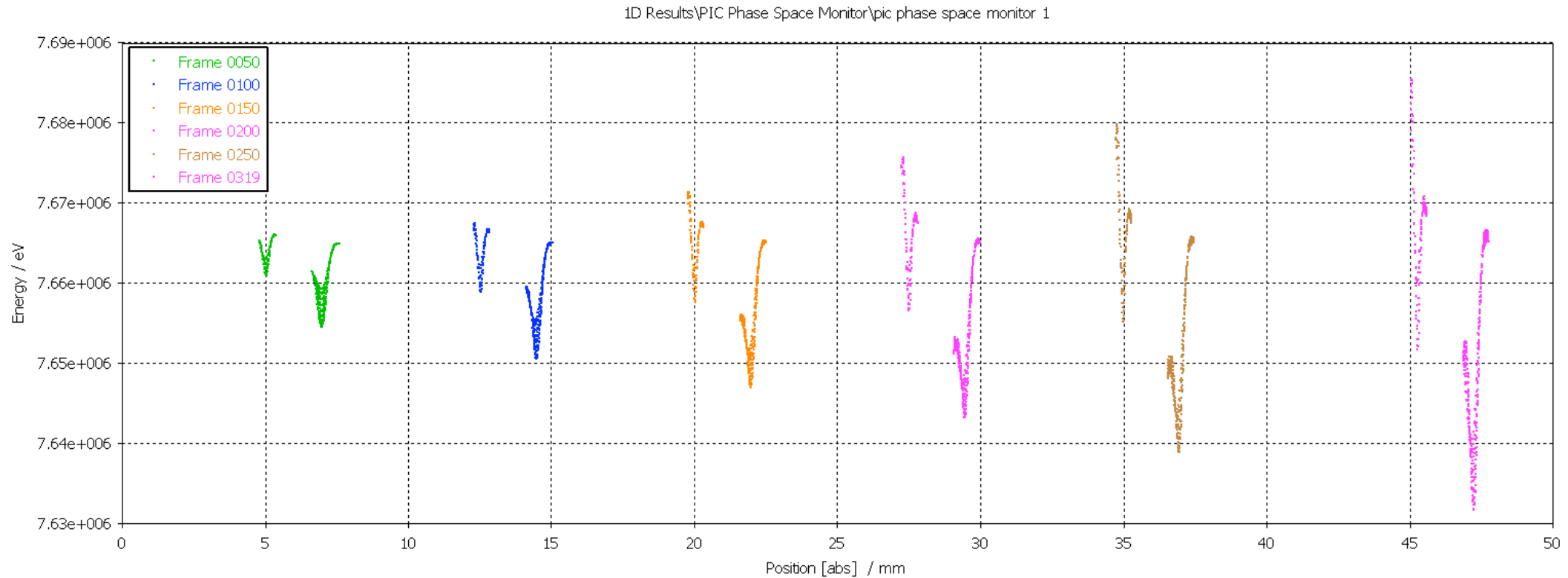
e-field (t=0.02, x=0) [pic]
Component: Abs
Cutplane normal: 1, 0, 0
Cutplane position: 0
Sample(0): 2
Time [ns]: 0.02



e-field (t=0.02, x=0) [pic]
Component: Abs
Cutplane normal: 1, 0, 0
Cutplane position: 7
Sample(0): 7
Time [ns]: 0.12

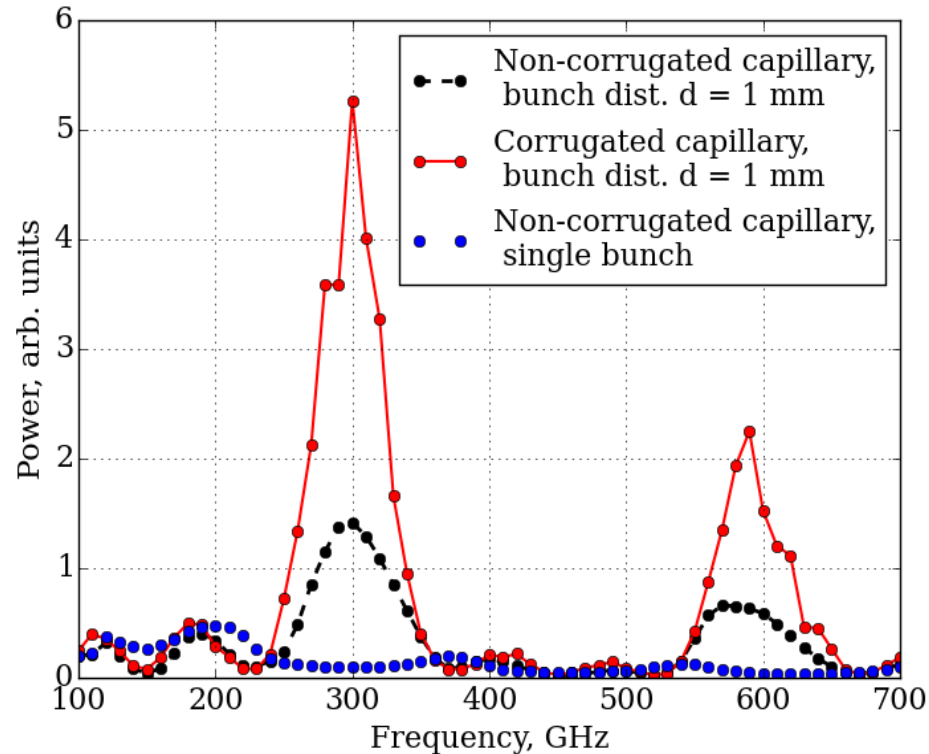
PIC simulations Drive-Witness experiment (new geometry)

- PIC simulation example for Drive (100pC) and Witness (20pC) separated by two corrugation periods propagating through the capillary centre.
- ~20 keV energy gain for given parameters (non-optimized).



Additional slides

PIC simulations multi-bunch (capillary with reflector)



Resonant condition:

bunch distance = corrugation period

The power radiated through the surface of the outside boundary A of the calculation domain during the simulation time Δt at each frequency is given by the following expression:

$$P(\omega) = \left| \int_0^{\Delta t} \oint \mathbf{S}(\omega) * \mathbf{n} dA dt \right|;$$

where $\mathbf{S}(\omega)$ is the Poynting vector, \mathbf{n} is a unity vector in the outward normal direction from the boundary A of the calculation domain.

Single bunch:

relatively flat response at all frequencies.

Blank capillary:

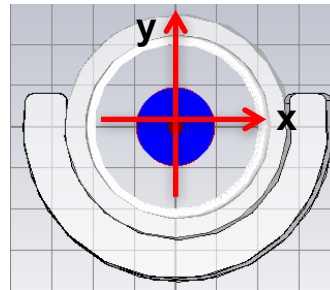
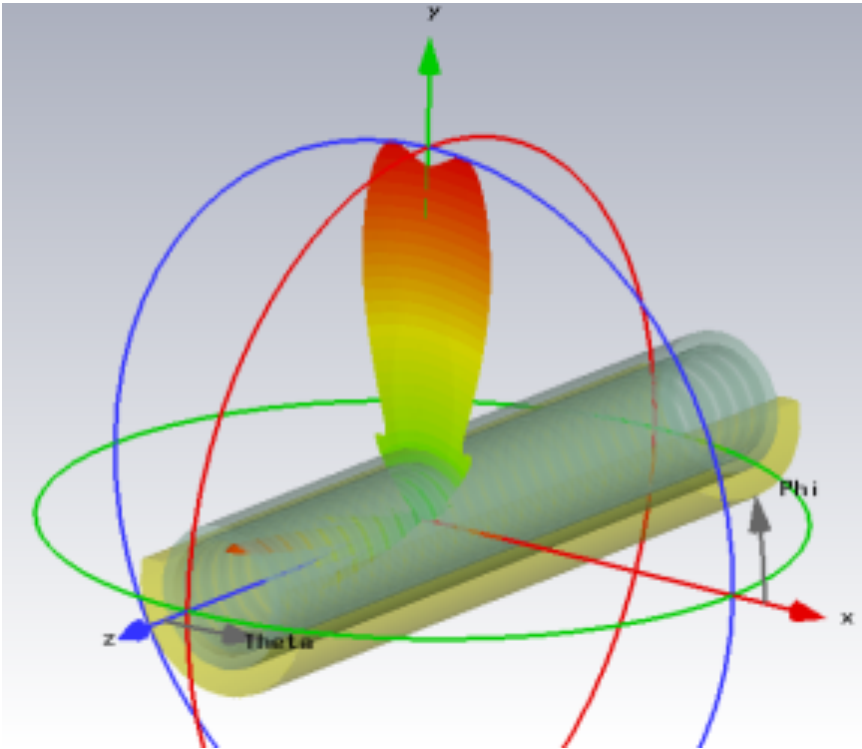
power spectral modulation due to Cherenkov radiation.

Corrugated capillary:

even larger spectral modulation if the distance between bunches is equal to the corrugation period.

PIC simulations (ChSPR)

- 3D power pattern and the corresponding azimuthal cross-sections ($\theta = 90$ deg.) for the radiation at 300 GHz for the off-central beam propagation $x=0$, $y=1$ mm.
- Cherenkov radiation is reflected by the outside boundaries of the corrugated capillary and directed at small angles $\theta \approx 10$ deg.



$$P_{peak} = \frac{P(\omega)}{\Delta t},$$

$\Delta t = 0.13$ ns
(simulation time)

